

Negative thermal expansion and local lattice distortion in the $(\text{Sc}_{1-x}\text{Ti}_x)\text{F}_3$ and related solid solutions

Xiaojian Wang,¹ Jun Chen,^{1,†} Fei Han,¹ Yang Ren,² Tao Wang,¹ Jinxia Deng,¹ and Xianran Xing¹

¹Department of Physical Chemistry, University of Science and Technology Beijing, Beijing 100083, China

²Argonne National Laboratory, X-Ray Science Division, Argonne, Illinois 60439, USA

[†]Corresponding Author, Electronic mail: Junchen@ustb.edu.cn

Abstract:

Negative thermal expansion (NTE) is unusual but important property for control of thermal expansion. In the present study, the chemical modification is utilized to engineer controllable thermal expansion in cubic NTE ScF_3 . A broad window of the coefficient of thermal expansion (CTE, $\alpha_1 = -1.51 \sim -3.4 \times 10^{-6} \text{ K}^{-1}$, 300-800 K) has been achieved in $\text{Sc}_{1-x}\text{M}_x\text{F}_3$ ($M = \text{Ti, Al and Ga}$). The long-range crystallographic structure of $(\text{Sc}_{1-x}\text{Ti}_x)\text{F}_3$ adheres to the cubic $Pm\bar{3}m$ symmetry according to the analysis of high-energy synchrotron X-ray powder diffraction. Pair distribution function (PDF) analysis of synchrotron X-ray total scattering was performed to investigate the local lattice distortion. It was found that the weakness of NTE has a close correlation with the local lattice distortion. Based on the coupled rotation model, it is presumably that this local distortion might dampen the transverse vibration of F atoms and thus reduce NTE. The present work provides a possible reference for the design of controllable NTE in open framework solids.

1. Introduction

Negative thermal expansion (NTE) is an interesting physical property of solid state chemistry, which is extensively applied in various functional materials.¹ A large amount of work have been conducted to explore controllable thermal expansion materials, such as ZrW_2O_8 ,² Invar alloys,³ NZP family,⁴ PbTiO_3 -based ferroelectrics,⁵⁻⁶ anti-perovskite nitrides,⁷ BiNiO_3 -based solid solutions,⁸ and ReO_3 -type fluorides.⁹⁻¹⁶ Among them, ScF_3 exhibits an intriguing isotropic NTE behavior, due to its simple structure with cubic corner-shared octahedra. There have several studies to elucidate the NTE and physical properties through chemical modification in ScF_3 like $(\text{Sc}_{1-x}\text{M}_x)\text{F}_3$ ($M = \text{Al}$,¹³ Y ,¹⁴ Fe ,¹⁵ Ti ,¹⁶ etc.). It has been found there is a certain correlation between the controllable thermal expansion with the local lattice distortion in the ScF_3 based solid solutions.^{11, 17}

In the present study, the chemically substituted ScF_3 solid solutions of $(\text{Sc}_{1-x}\text{M}_x)\text{F}_3$ ($M = \text{Ti}$, Al , and Ga) have been prepared. A tunable thermal expansion was observed in these isotropic ScF_3 -based systems. Interestingly, the coefficient of thermal expansion (CTE) of $(\text{Sc}_{1-x}\text{M}_x)\text{F}_3$ is found to show a close relationship with the degree of local lattice distortion. Such lattice distortion presumably could restrain the transverse motion of fluorine atoms, and thus weakens NTE. The present work could be helpful for the design of thermal expansion in NTE compounds

through chemical modification.

2. Result and Discussion

The details of Experimental section are given in the Supporting Information (SI). As shown in Fig. S1, ScF₃ exhibits a cubic ReO₃-type framework structure which is composed of corner-sharing ScF₆ octahedra. Structure refinements have been performed to determine crystal structure of (Sc_{1-x}Ti_x)F₃ solid solutions, (Sc_{0.9}Al_{0.1})F₃, and (Sc_{0.9}Ga_{0.1})F₃ (Fig. 1, Fig. S3 and Fig. S4). It is found that the crystal structure of all compositions maintains cubic $Pm\bar{3}m$ symmetry, in which F atoms are located at the 3d site (0.5, 0, 0) and metal atoms at the 1a site (0, 0, 0). Fig. S2 shows lattice parameters as function of Ti content (x). One can see that the lattice parameter, a , decreases with increasing content of Ti (x). It is 4.0115(1) Å for ScF₃ and 3.9350(1) Å for (Sc_{0.1}Ti_{0.9})F₃. The decrease in lattice parameters is in a good agreement with the decrease in ionic radius for Sc³⁺ (0.745 Å) and Ti³⁺ (0.670 Å).¹⁸

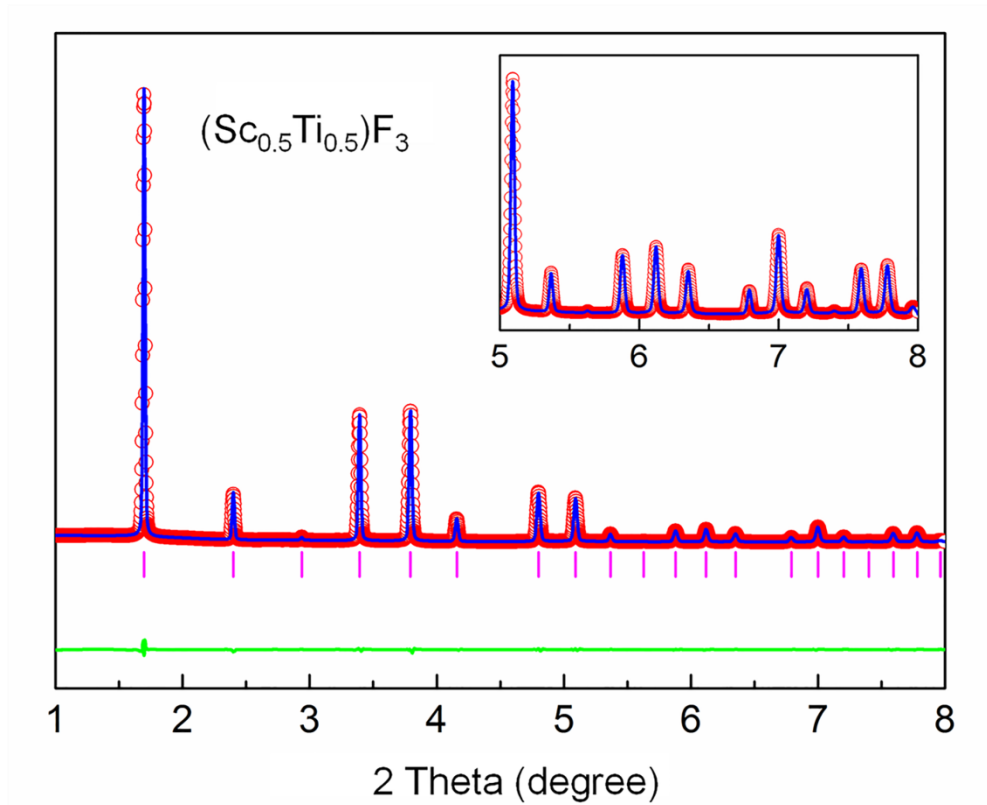


Figure 1. Observed, calculated, difference of patterns of structure refinement of $(\text{Sc}_{0.5}\text{Ti}_{0.5})\text{F}_3$ from high-energy synchrotron X-ray diffraction data.

As shown in Fig. 2a, the temperature dependence of lattice parameters exhibits a distinct thermal expansion as a function of TiF_3 content. The magnitude of NTE differs noticeably from strong NTE of ScF_3 to weak NTE of $(\text{Sc}_{0.1}\text{Ti}_{0.9})\text{F}_3$.

Fig. 2b provides linear CTEs of $(\text{Sc}_{1-x}\text{Ti}_x)\text{F}_3$ solid solutions as a function of Ti content (x). From room temperature to 800 K, ScF_3 exhibits a relatively strong NTE with an average linear CTE of $-3.4 \times 10^{-6} \text{ K}^{-1}$, which is in accordance with the value of $-3.0 \times 10^{-6} \text{ K}^{-1}$ in the previous study.⁹ By chemical substitution of 50 mol% Ti^{3+} for Sc^{3+} , i.e., $(\text{Sc}_{0.5}\text{Ti}_{0.5})\text{F}_3$, its NTE is weakened ($\alpha_1 = -2.94 \times 10^{-6} \text{ K}^{-1}$, 300-800 K).

With further chemical substitution, thermal expansion of $(\text{Sc}_{0.1}\text{Ti}_{0.9})\text{F}_3$ develops less negative ($\alpha_1 = -1.51 \times 10^{-6} \text{ K}^{-1}$, 300-800 K). As a conclusion, one can see that NTE of $(\text{Sc}_{1-x}\text{Ti}_x)\text{F}_3$ becomes more and more weakened with chemical substitution of Sc by Ti atom. Here, a nearly continuous isotropic CTEs are achieved in $(\text{Sc}_{1-x}\text{Ti}_x)\text{F}_3$. The solid solutions functionalize over a wide temperature range, especially including the high temperature up to 800K. Until now, high-temperature isotropic NTE is rare, such as $\text{Zr}_{1-x}\text{Sn}_x\text{Mo}_2\text{O}_8$,¹⁹ TaO_2F ,²⁰ $M\text{ZrF}_6$.²¹ This present system of $(\text{Sc}_{1-x}\text{Ti}_x)\text{F}_3$ extends the diversity of high-temperature isotropic NTE species.

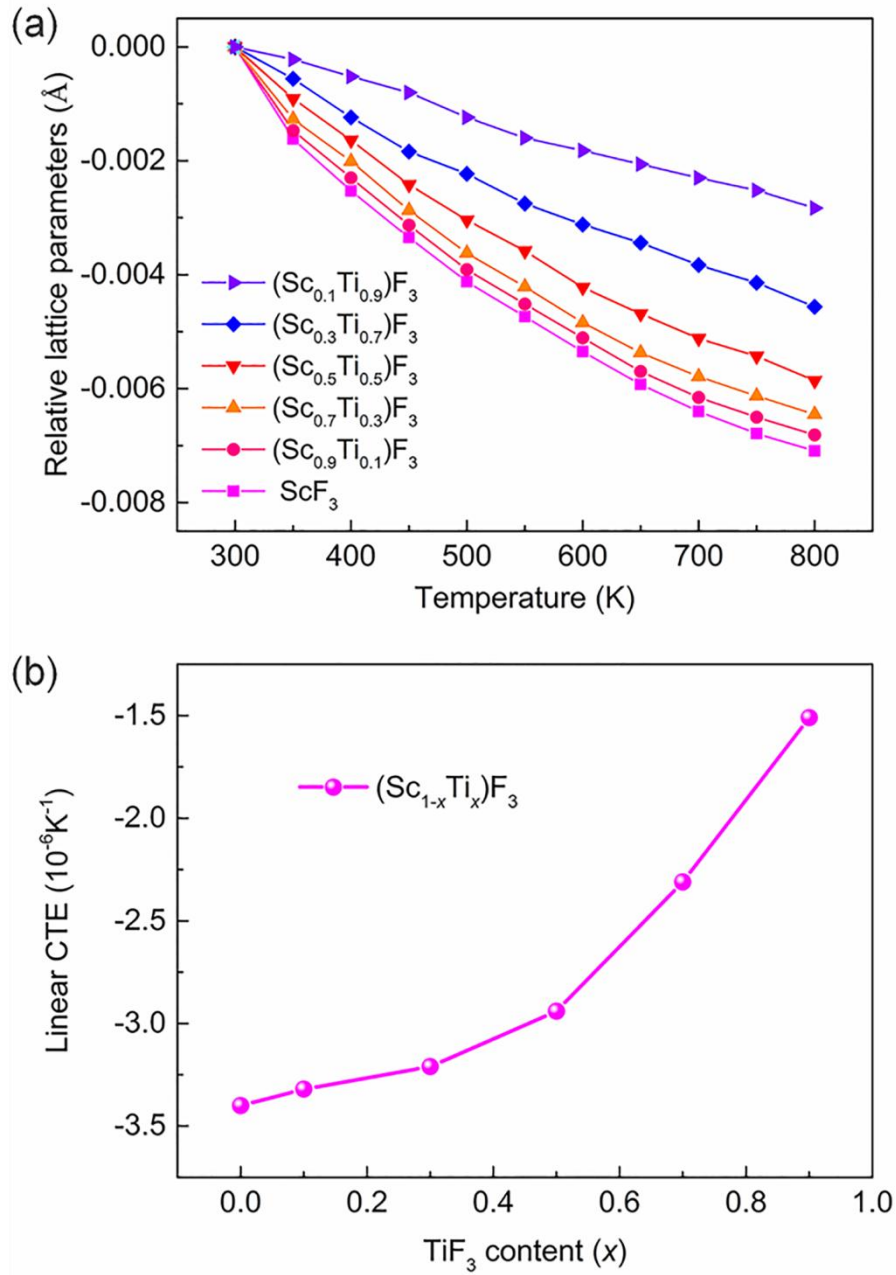


Figure 2. (a) Temperature-dependence variation of relative lattice parameters, and (b) linear CTE of $(\text{Sc}_{1-x}\text{Ti}_x)\text{F}_3$ ($x = 0, 0.1, 0.3, 0.5, 0.7,$ and 0.9) solid solutions.

Synchrotron X-ray diffraction (SXRD) result shows that all present ScF_3 -based solid solutions remain cubic symmetry macroscopically. If not, several apparent peaks due to symmetry breaking would appear in

the SXRD patterns, like depicted in Figure S5. However, local lattice distortions could be responsible for the difference in thermal expansion. It is essential to further explore local lattice distortions. Here, we have performed the atomic pair distribution function (PDF) analysis of synchrotron radiation X-ray total scattering for the present ScF₃-based solid solutions (Fig. 3a, Fig. S6, and Fig. S7).

Firstly in order to be consistent with the XRD results, the cubic $Pm\bar{3}m$ model was adopted to investigate the local lattice distortion at the initial attempts. But unsatisfactorily, the fitting results indicate that the cubic model cannot match the experimental PDF data well. It could be anticipated that local lattice distortions certainly appear with the chemical substitutions of Ti³⁺, Al³⁺ or Ga³⁺ for Sc³⁺. Therefore, enlightened by the documentation that the ReO₃-type metal trifluorides commonly retain in $R\bar{3}c$ symmetry (such as AlF₃), it could be reasonable to utilize a rhombohedral $R\bar{3}c$ model to investigate the local structure. Based on this model, the refinement obtains quite acceptable fitting results. PDF analyses demonstrate that the rhombohedral model is superior to the cubic counterpart at the low r range (1.7-20 Å) (Fig. S8).

It was previously reported that ScF₃ adopts the cubic ReO₃ structure in which the Sc–F–Sc linkages are straight.¹⁰ Related to the strong coupling rotation of ScF₆ octahedral units, the transverse vibration of F atom perpendicular to the straight Sc··Sc axis results in a decrease in

Sc ···Sc distance and thus the strong NTE.¹⁰ However, for the distorted rhombohedral model, a certain displacement exists in F atoms deviating from its original central location and leading to bent M-F-M (M = Ti, Al, Ga) linkages with a value of θ less than 180° (Fig. 3b). Here, the difference, $\Delta\theta = 180^\circ - \theta$, is defined as the distortion degree.

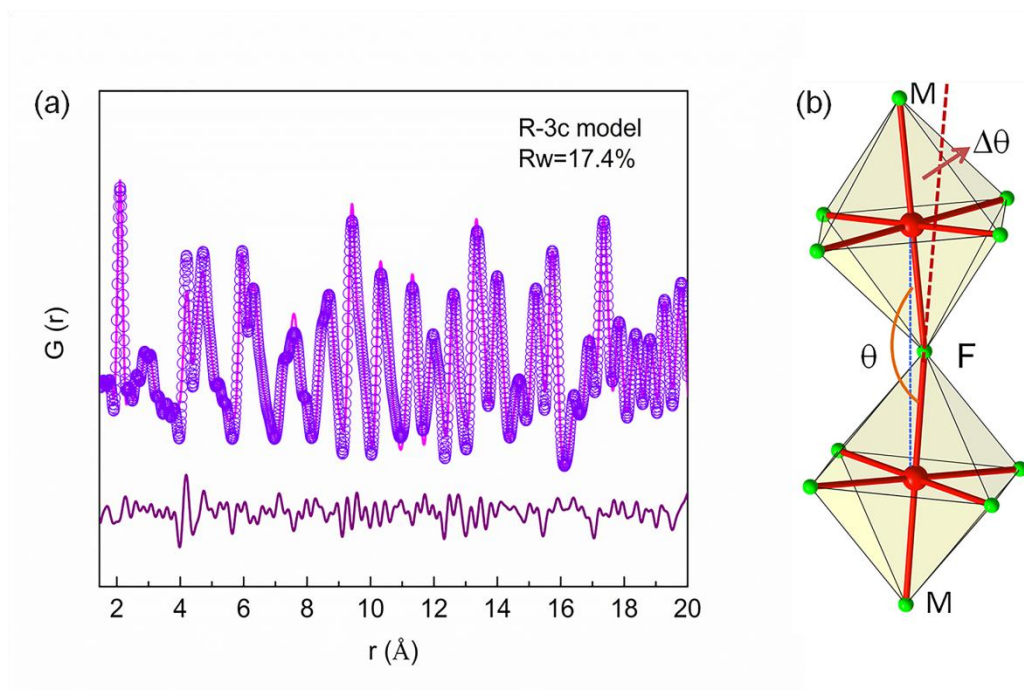


Figure 3. (a) Pair distribution function (PDF) fit of synchrotron X-ray scattering obtained at 300 K for $(\text{Sc}_{0.5}\text{Ti}_{0.5})\text{F}_3$ with the rhombohedral model at low r (1.7–20 Å). The violet circles and red line correspond to the experimental and calculated data, respectively. Difference curve is shown by the purple line at the bottom. (b) The angle of M - F - M linkage, θ , extracted from the rhombohedral model which was used to fit to the PDF data of $(\text{Sc}_{1-x}\text{M}_x)\text{F}_3$ system ranging from 1.7–20 Å.

In order to elucidate the correlation between the behavior of thermal expansion and local lattice distortion, Fig. 4 depicts the CTE data as a function of distortion degree of $\Delta\theta$ for ScF_3 -based compounds and those

representative trifluorides. The specific data are summarized in Table S1. Intriguingly, a close correlation is demonstrated clearly between local structure distortion and thermal expansion. With increasing local lattice distortion, NTE of $(\text{Sc}_{1-x}\text{M}_x)\text{F}_3$ becomes more and more reduced. In details, with the chemical substitution of TiF_3 for ScF_3 , the CTE changes from $-3.4 \times 10^{-6} \text{ K}^{-1}$ for ScF_3 to $-1.51 \times 10^{-6} \text{ K}^{-1}$ for $(\text{Sc}_{0.1}\text{Ti}_{0.9})\text{F}_3$, of which the distortion degree simultaneously changes from 4.21° to 6.33° . To summarize, they are all well in accordance with this relationship including the present solid solutions of $(\text{Sc}_{1-x}\text{Ti}_x)\text{F}_3$, $(\text{Sc}_{0.9}\text{Al}_{0.1})\text{F}_3$, $(\text{Sc}_{0.9}\text{Ga}_{0.1})\text{F}_3$, and the other previously reported compounds¹⁷.

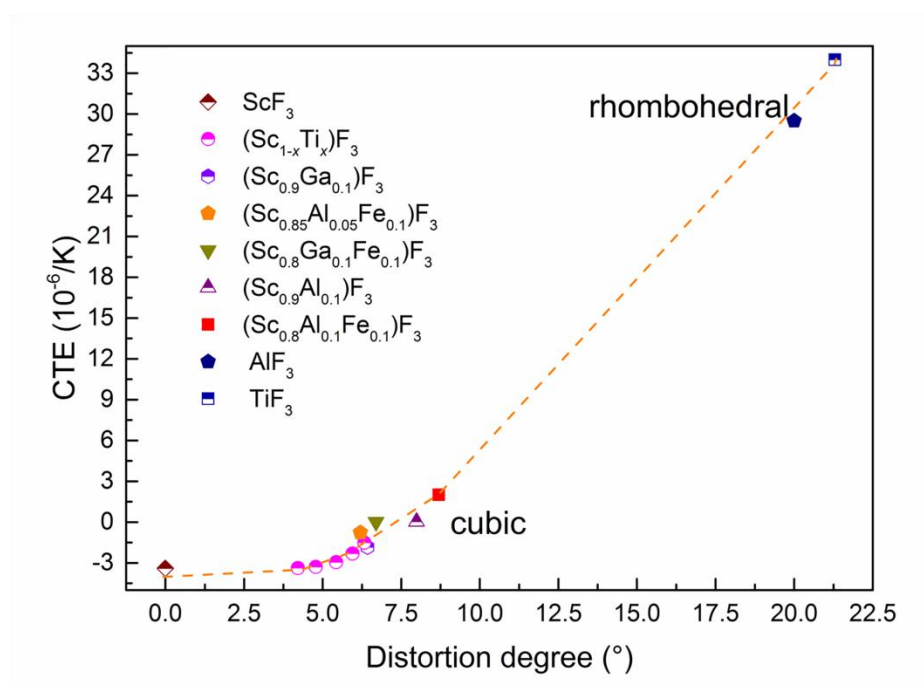


Figure 4. The correlation between local lattice distortion and CTE for ScF_3 -based compounds and other representative trifluorides. The data of $(\text{Sc}_{0.85}\text{Al}_{0.05}\text{Fe}_{0.1})\text{F}_3$, $(\text{Sc}_{0.8}\text{Ga}_{0.1}\text{Fe}_{0.1})\text{F}_3$, $(\text{Sc}_{0.85}\text{Al}_{0.05}\text{Fe}_{0.1})\text{F}_3$ and AlF_3 are adopted from the literature.¹⁷

It can be expected that after the introduction of local lattice

distortion transverse vibration of F atoms would contribute less to NTE but more to positive thermal expansion (PTE) component. The previous work has already claimed that the NTE behavior is favored by the straight M-X-M linkage (here X and M indicate anion and cation, respectively)²⁰. And the bent M-X-M linkage tends to give rise to PTE. This is confirmed by rhombohedral metal fluorides showing very strong PTE (Fig. 4), in which the M-F-M linkage is much bent, like TiF₃ and AlF₃ (the angle of Ti-F-Ti is 157.9 ° and that of Al-F-Al is 159 °)¹⁷. In the previous work of Sc_{1-x}M_xF₃ (M = Ga, Fe; Al, Fe)^{11,17}, the controllable thermal expansion was also found to be correlated with the distortion of M-F-M linkages. Thus, controllable thermal expansion can be achieved if local lattice distortion is appropriately adjusted by different substitutions.

3. Conclusion

The solid solutions of (Sc_{1-x}Ti_x)F₃ ($x = 0.1, 0.3, 0.5, 0.7,$ and 0.9), (Sc_{0.9}Al_{0.1})F₃, and (Sc_{0.9}Ga_{0.1})F₃ were synthesized to study the correlation between local lattice distortion and thermal expansion. By the chemical substitution of TiF₃ for ScF₃, the thermal expansion behavior of (Sc_{1-x}Ti_x)F₃ becomes less and less negative. Different from cubic ScF₃, there are local lattice distortions in solid solutions of (Sc_{1-x}Ti_x)F₃, (Sc_{0.9}Al_{0.1})F₃, and (Sc_{0.9}Ga_{0.1})F₃. The relationship between thermal expansion and local lattice distortion is elucidated clearly. The larger local lattice distortion is, the more reduced NTE becomes. The present

study could provide an effective method to control thermal expansion for those NTE materials with open-framework structure.

Acknowledgements

This work was supported by the National Natural Science Foundation of China (grant nos. 21322102, 91422301, 21231001, and 21590793), the Changjiang Young Scholars Award, National Program for Support of Top-notch Young Professionals, and the Fundamental Research Funds for the Central Universities, China (FRF-TP-14-012C1). This research used resources of the Advanced Photon Source, a U.S. Department of Energy (DOE) Office of Science User Facility operated for the DOE Office of Science by Argonne National Laboratory under Contract No. DE-AC02-06CH11357.

References

- 1 J. Chen, L. Hu, J. Deng, and X. Xing, "Negative thermal expansion in functional materials: controllable thermal expansion by chemical modifications," *Chem. Soc. Rev.*, **44**, 3522-67 (2015).
- 2 T. Mary, J. Evans, T. Vogt, and A. Sleight, "Negative thermal expansion from 0.3 to 1050 Kelvin in ZrW_2O_8 ," *Science*, **272**, 90-2 (1996).
- 3 P. Mohn, "A century of zero expansion," *Nature*, **400**, 18-9 (1999).
- 4 R. Roy, D. K. Agrawal, and H. A. McKinstry, "Very low thermal expansion coefficient materials," *Ann. Rev. Mater. Sci.*, **19**, 59-81 (1989).
- 5 J. Chen, K. Nittala, J. S. Forrester, J. L. Jones, J. Deng, R. Yu, and X. Xing, "The role of spontaneous polarization in the negative thermal expansion of tetragonal $PbTiO_3$ -based compounds," *J. Am. Chem. Soc.*, **133** [29] 11114-7 (2011).
- 6 J. Chen, L. Fan, Y. Ren, Z. Pan, J. Deng, R. Yu, and X. Xing, "Unusual transformation from strong negative to positive thermal expansion in $PbTiO_3$ - $BiFeO_3$ Perovskite," *Phys. Rev. Lett.*, **110**, 115901-5 (2013).
- 7 K. Takenaka and H. Takagi, "Giant negative thermal expansion in Ge-doped anti-perovskite manganese nitrides," *Appl. Phys. Lett.*, **87**, 261902-4 (2005).
- 8 M. Azuma, W. T. Chen, H. Seki, M. Czapski, K. Oka, M. Mizumaki, T.

Watanuki, N. Ishimatsu, N. Kawamura, and S. Ishiwata, “Colossal negative thermal expansion in BiNiO₃ induced by intermetallic charge transfer,” *Nat. Commun.*, **2**, 347-5 (2011).

9 B. K. Greve, K. L. Martin, P. L. Lee, P. J. Chupas, K. W. Chapman, and A. P. Wilkinson, “Pronounced negative thermal expansion from a simple structure: cubic ScF₃,” *J. Am. Chem. Soc.*, **132** [44] 15496-8 (2010).

10 L. Hu, J. Chen, A. Sansons, H. Wu, C. G. Rodriguez, L. Olivi, Y. Ren, L. L. Fan, J. X. Deng, and X. R. Xing, “New insights into the negative thermal expansion: direct experimental evidence for the ‘guitar-string’ effect in cubic ScF₃,” *J. Am. Chem. Soc.*, **138**, 8320-3 (2016).

11 L. Hu, J. Chen, L. Fan, Y. Ren, Y. Rong, Z. Pan, J. Deng, R. B. Yu, and X. R. Xing, “Zero thermal expansion and ferromagnetism in cubic Sc_{1-x}M_xF₃ (M = Ga, Fe) over a wide temperature range,” *J. Am. Chem. Soc.*, **136** [39] 13566-9 (2014).

12 L. Hu, J. Chen, L. L. Fan, J. X. Deng, R. B. Yu, and X. R. Xing, “Rapid molten salt synthesis of isotropic negative thermal expansion ScF₃,” *J. Am. Ceram. Soc.*, **97** [4] 1009-11 (2014).

13 C. R. Morelock, L. C. Gallington, and A. P. Wilkinson, “Solid solubility, phase transitions, thermal expansion, and compressibility in Sc_{1-x}Al_xF₃,” *J. Solid State Chem.*, **222**, 96-102 (2015).

14 C. R. Morelock, B. K. Greve, L. C. Gallington, K. W. Chapman, and

A. P. Wilkinson, “Negative thermal expansion and compressibility of $\text{Sc}_{1-x}\text{Y}_x\text{F}_3$ ($x \leq 0.25$),” *J. Appl. Phys.*, **114**, 213501-8 (2013).

15 L. Hu, J. Chen, L. Fan, Y. Ren, Q. Huang, A. Sanson, Z. Jiang, M. Zhou, Y. Rong, and Y. Wang, “High - Curie - temperature ferromagnetism in $(\text{Sc,Fe})\text{F}_3$ fluorides and its dependence on chemical valence,” *Adv. Mater.*, **27** [31] 4592-6 (2015).

16 C. R. Morelock, L. C. Gallington, and A. P. Wilkinson, “Evolution of negative thermal expansion and phase transitions in $\text{Sc}_{1-x}\text{Ti}_x\text{F}_3$,” *Chem. Mater.*, **26** [5] 1936-40 (2014).

17 F. Han, J. Chen, L. Hu, Y. Ren, Y. Rong, Z. Pan, J. X. Deng, and X. R. Xing, “The distortion-adjusted change of thermal expansion behavior of cubic magnetic semiconductor $(\text{Sc}_{1-x}\text{M}_x)\text{F}_3$ ($M = \text{Al}, \text{Fe}$),” *J. Am. Ceram. Soc.*, **99**, 2886-9 (2016).

18 R. Shannon, “Revised effective ionic radii and systematic studies of interatomic distances in halides and chalcogenides,” *Acta Crystallogr., Sect. A* **32** [5], 751–7 (1976).

19 S. E. Tallentire, F. Child, and I. Fall, “Systematic and controllable negative, zero, and positive thermal expansion in cubic $\text{Zr}_{1-x}\text{Sn}_x\text{Mo}_2\text{O}_8$,” *J. Am. Ceram. Soc.*, **44** [34] 12849-56 (2013).

20 Tao J Z, Sleight A W, “The role of rigid unit modes in negative

thermal expansion,” *J. Solid State Chem.*, **173** [2] 442-8 (2003).

21 L. Hu, J. Chen, J. Xu., N. Wang, F. Han, Y. Ren, Z. Pan, Y. C. Rong, R. J. Huang, J. X. Deng, L. F. Li, and X. R. Xing “Atomic linkage flexibility tuned isotropic negative, zero, and positive thermal expansion in $MZrF_6$ ($M = Ca, Mn, Fe, Co, Ni, \text{ and } Zn$),” *J. Am. Chem. Soc.*, **138** [44] 14530-3 (2016).

Supporting Information for “Negative thermal expansion and local lattice distortion in the $(\text{Sc}_{1-x}\text{Ti}_x)\text{F}_3$ and related solid solutions”

Experimental section

The samples were prepared via a solid state synthesis route. The raw materials of ScF_3 (99.99%), TiF_3 (98%), AlF_3 (99.9%), GaF_3 (99.99%) and NH_4F (99.99%) powders, were mixed according to the stoichiometric starting reagents of $(\text{Sc}_{1-x}\text{Ti}_x)\text{F}_3$, $(\text{Sc}_{0.9}\text{Al}_{0.1})\text{F}_3$, and $(\text{Sc}_{0.9}\text{Ga}_{0.1})\text{F}_3$. These mixtures were pressed into small pellets which were then sandwiched into additional NH_4F powder. Then the samples were sealed carefully into Cu tubes in order to avoid oxidization. Subsequently, these samples were heated at 850 °C for 2 h under ambient condition, before they were gradually cooled to room temperature. High-energy synchrotron X-ray diffraction (SXRD) data were collected over an angular range of 1-8° at the beamline 11-ID-C at the Advanced Photon Source (APS). The X-ray wavelength was $\lambda = 0.117418 \text{ \AA}$. The synchrotron X-ray scattering data for pair distribution function (PDF) were also collected at the same beamline of 11-ID-C of APS with the identical X-ray wavelength ($\lambda = 0.117418 \text{ \AA}$). All these X-ray scattering data were analyzed using the software of PDFgetX3,¹ and structure refinements were achieved by PDFgui.² Temperature-dependence of XRD data were collected from 300 to 900 K using a laboratory X-ray diffractometer (PANalytical, PW

3040-X'PertPro). The cubic ($Pm\bar{3}m$) model was adopted for the Rietveld refinement based on *Fullprof* software.

Results and discussion

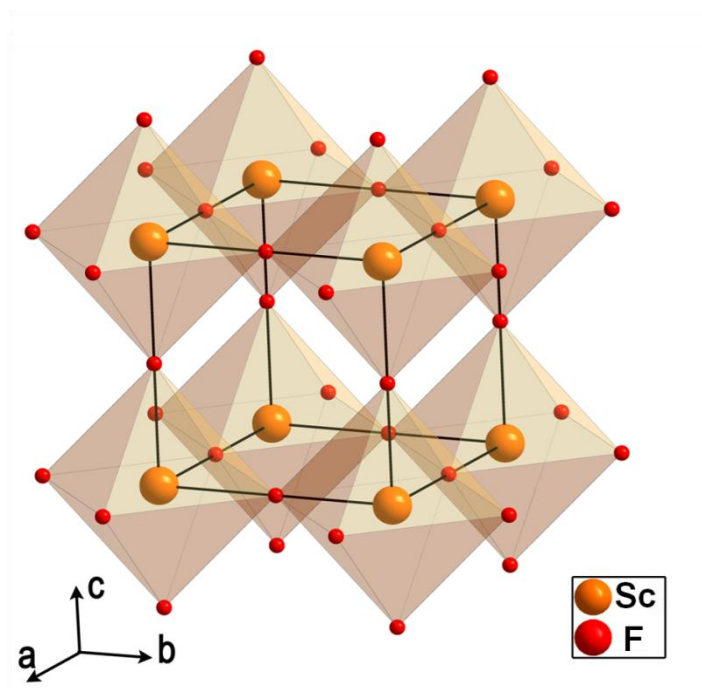


Figure S1. Crystal structure of cubic ScF₃.

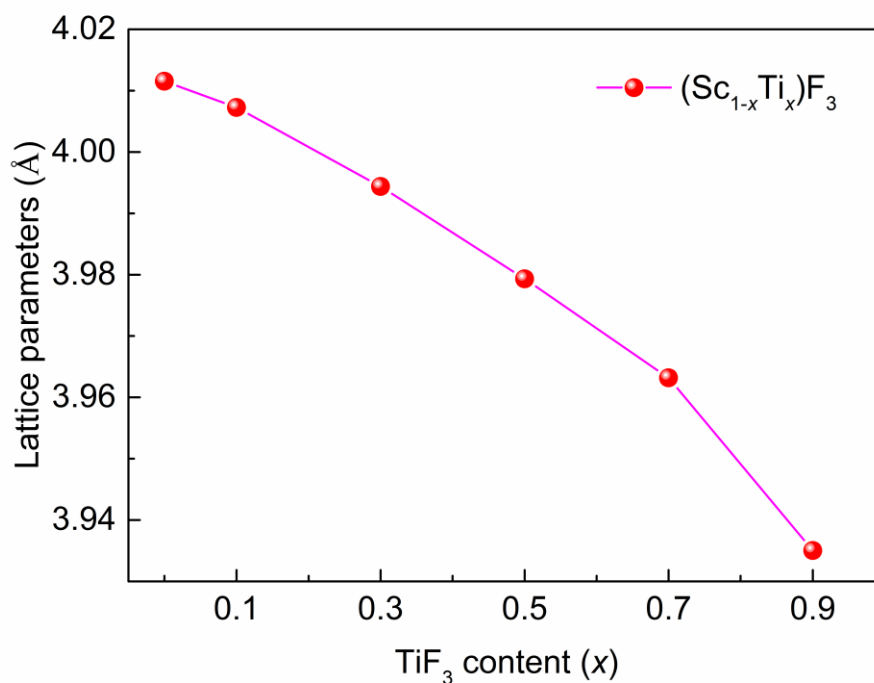


Figure S2. Lattice parameters of (Sc_{1-x}Ti_x)F₃ ($x = 0, 0.1, 0.3, 0.5, 0.7$ and 0.9) solid solutions at room temperature.

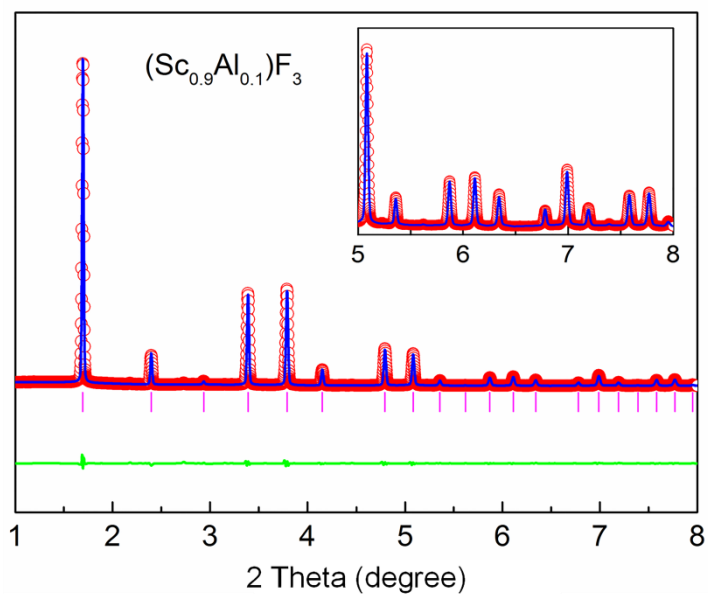


Figure S3. Observed, calculated, difference patterns of structure refinements of high-energy synchrotron XRD data of $(\text{Sc}_{0.9}\text{Al}_{0.1})\text{F}_3$.

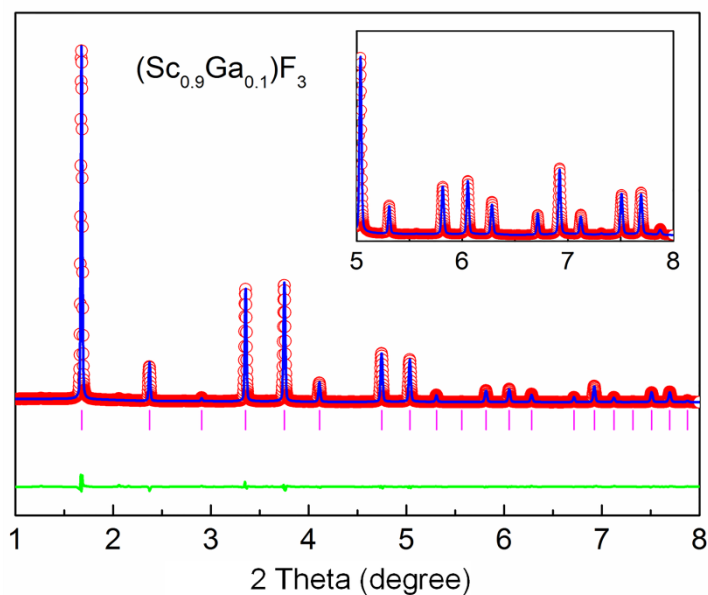


Figure S4. Observed, calculated, difference patterns of structure refinements of high-energy synchrotron XRD data of $(\text{Sc}_{0.9}\text{Ga}_{0.1})\text{F}_3$.

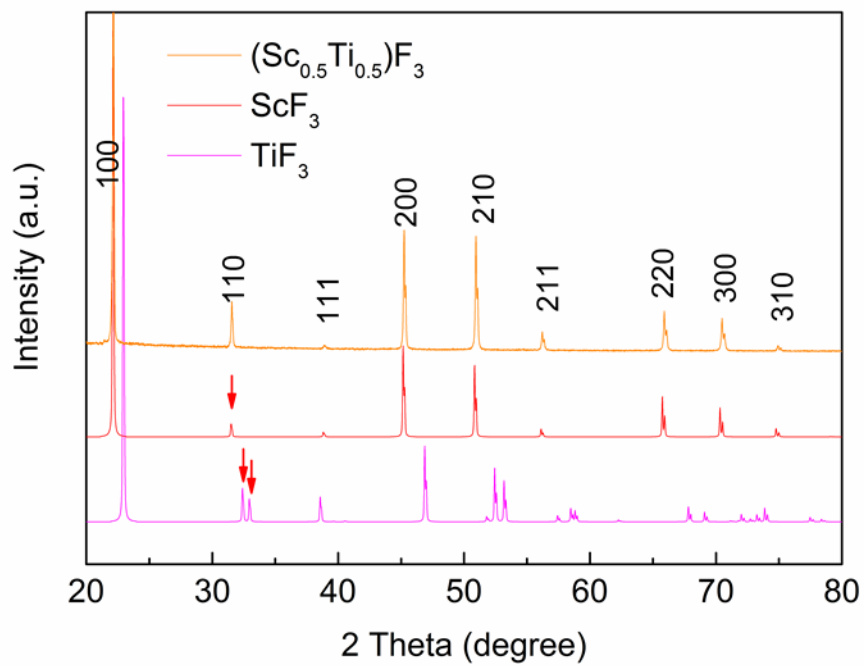


Figure 5. The XRD patterns of the $(\text{Sc}_{0.5}\text{Ti}_{0.5})\text{F}_3$ sample with $R\bar{3}c$ TiF_3 and $Pm\bar{3}m$ ScF_3 standard cards.

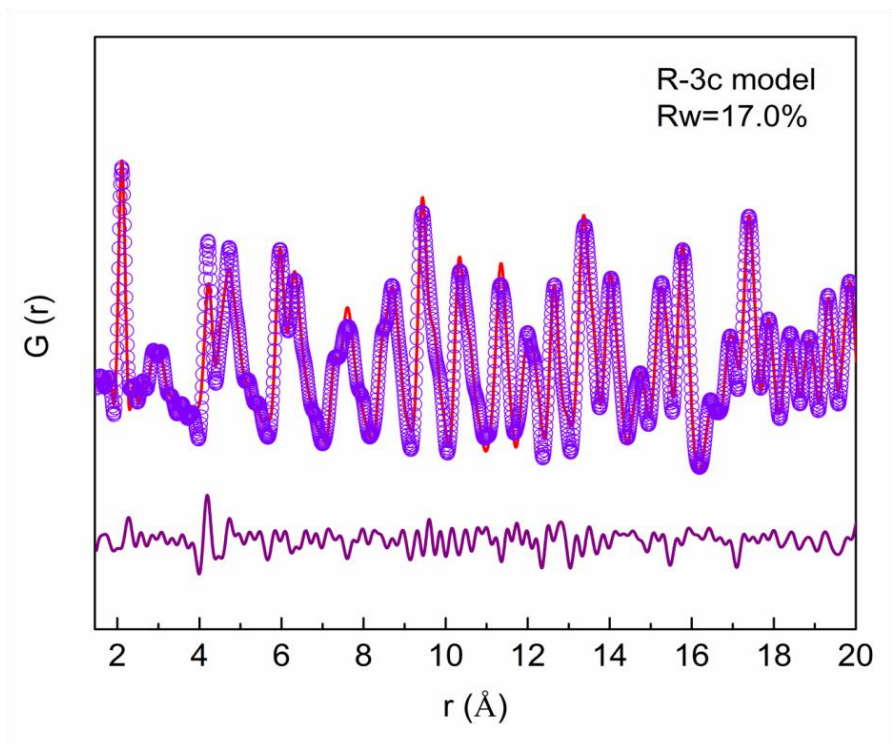


Figure S6. Pair distribution function (PDF) fit of synchrotron X-ray scattering obtained at room temperature for $(\text{Sc}_{0.9}\text{Al}_{0.1})\text{F}_3$ with the rhombohedra model at low r (1.7-20 \AA). The violet circles and red line correspond to the experimental and calculated data, respectively. Difference curve is shown by the purple line at the bottom.

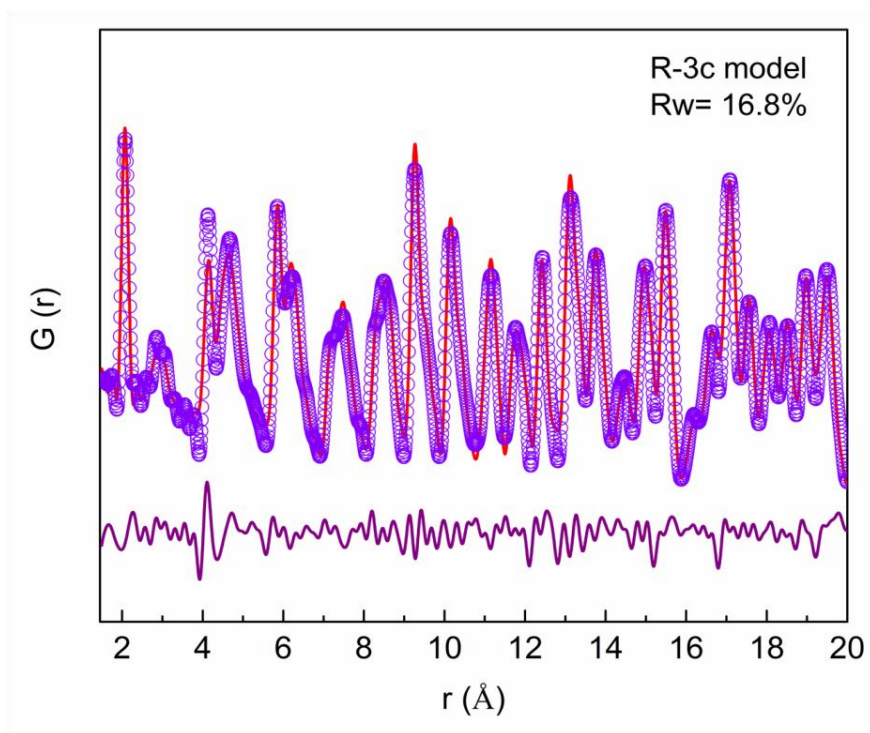


Figure S7. Pair distribution function (PDF) fit of synchrotron X-ray scattering obtained at room temperature for $(\text{Sc}_{0.9}\text{Ga}_{0.1})\text{F}_3$ with the rhombohedra model at low r (1.7-20 \AA). The violet circles and red line correspond to the experimental and calculated data, respectively. Difference curve is shown by the purple line at the bottom.

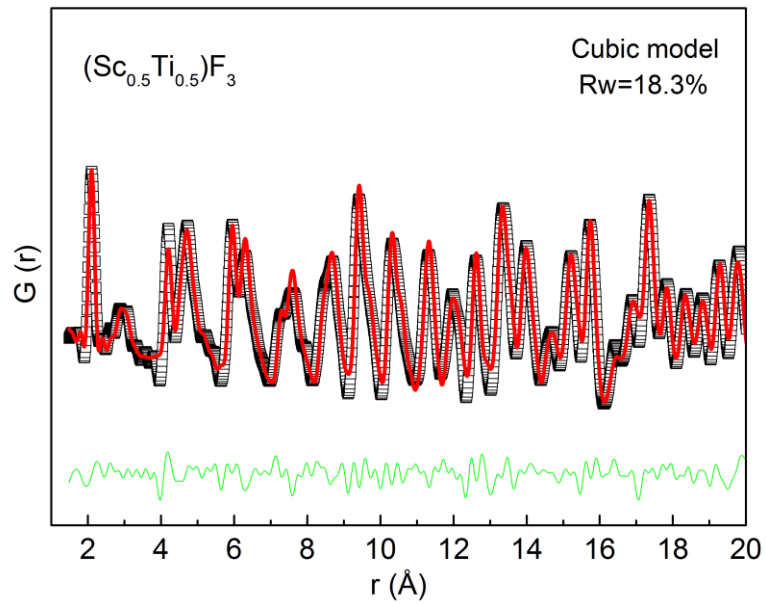


Figure S8. Pair distribution function (PDF) fit of synchrotron X-ray scattering $G(r)$ functions for $(\text{Sc}_{0.5}\text{Ti}_{0.5})\text{F}_3$ with cubic model. The black squares and the red line represent the observed data and the fitted one, respectively. The green line at the bottom indicates the difference between the observed and fitted data.

Table S1. Thermal expansion and lattice distortion angles for ScF₃-based compounds and TiF₃.

Compounds	Angle of M-F-M (θ)	Distortion degree ($\Delta\theta$)	Linear CTE (10^{-6} K^{-1})	References
ScF ₃	180 °	0 °	-3.4	Ref. 3
(Sc _{0.9} Ti _{0.1})F ₃	175.8 °	4.2 °	-3.37	this study
(Sc _{0.7} Ti _{0.3})F ₃	175.2 °	4.8 °	-3.29	this study
(Sc _{0.5} Ti _{0.5})F ₃	174.6 °	5.4 °	-2.94	this study
(Sc _{0.3} Ti _{0.7})F ₃	174.1 °	6.0 °	-2.31	this study
(Sc _{0.1} Ti _{0.9})F ₃	173.7 °	6.3 °	-1.51	this study
(Sc _{0.9} Ga _{0.1})F ₃	173.6 °	6.4 °	-1.84	this study
(Sc _{0.9} Al _{0.1})F ₃	172.0 °	8.0 °	-0.53	this study
TiF ₃	157.9 °	21.3 °	36.0	Ref. 4

The temperature range of all ScF₃ based compounds is from 300 to 800 K.

That of TiF₃ ranges from 10 to 375 K.

References

- 1 P. Juhás, T. Davis, C. L. Farrow, and S. J. Billinge, “PDFgetX3: a rapid and highly automatable program for processing powder diffraction data into total scattering pair distribution functions,” *J. Appl. Crystallogr.*, **46** [2] 560-6 (2013).
- 2 C. Farrow, P. Juhas, J. Liu, D. Bryndin, E. Božin, J. Bloch, T. Proffen, and S. Billinge, “PDFfit2 and PDFgui: computer programs for studying nanostructure in crystals,” *J. Phys.: Condens. Matter*, **19** [33] 335219 (2007).
- 3 L. Hu, J. Chen, A. Sansons, H. Wu, C. G. Rodriguez, L. Olivi, Y. Ren, L. Fan, J. Deng, and X. Xing, “New insights into the negative thermal expansion: direct experimental evidence for the ‘guitar-string’ effect in cubic ScF_3 ,” *J. Am. Chem. Soc.*, **138**, 8320-3 (2016).
- 4 B. J. Kennedy and T. Vogt, “Powder X-ray diffraction study of the rhombohedral to cubic phase transition in TiF_3 ,” *Mater. Res. Bull.*, **37** [1] 77-83 (2002).